DISCOVERY OF RADIO JETS IN $z \sim 2$ ULTRALUMINOUS INFRARED GALAXIES WITH DEEP 9.7 μm SILICATE ABSORPTION

ANNA SAJINA,[1] LIN YAN,[1] MARK LACY,[1] AND MINH HUYNH[1]
Received 2007 July 6; accepted 2007 August 2; published 2007 August 31

ABSTRACT

Recent *Spitzer* observations have revealed a substantial population of $z \sim 2$ ultraluminous infrared galaxies (ULIRGs) with deep silicate absorption ($\tau_{9.7} > 1$). This paper reports a 20 cm radio study of such a sample to elucidate their physical nature. We discover that a substantial fraction (40%) of deep silicate absorption ULIRGs at $z \sim 2$ are moderately radio-loud, with $L_{1.4\text{GHz}} = 10^{25}$–$10^{26}$ W Hz^{-1}. This is in strong contrast with $z \lesssim 1$ radio galaxies and radio-loud quasars where none of the sources with available IRS spectra have $\tau_{9.7} > 1$. In addition, we observe radio jets in two of our sources, with one having a double lobe structure ~ 200 kpc in extent and the other showing a one-sided jet extending ~ 90 kpc from the nucleus. The likely high inclination of the latter, coupled with its deep silicate absorption, implies the mid-IR obscuration does not share an axis with the radio jets. These sources are highly obscured quasars, observed in the transition stage after the birth of the radio source, but before feedback effects dispel the interstellar medium and halt the black hole accretion and starburst activity.

Subject headings: galaxies: active — galaxies: high-redshift — galaxies: jets — infrared: galaxies — radio continuum: galaxies

1. INTRODUCTION

The local relationship between the bulge mass and black hole mass (Magorrian et al. 1998) suggests that the stellar mass build-up and black hole growth were coeval. This is supported by the number density evolution of quasars and radio galaxies (Wall et al. 2005; Richards et al. 2006a) being similar to the evolution of the star formation rate (SFR) density with redshift (e.g., Giavalisco et al. 2004). Observations of significant far-infrared (IR) emission potentially suggest starbursts associated with high-z quasars and radio galaxies (e.g., Willott et al. 2002; Reuland et al. 2003; Beelen et al. 2006) and indicate rapid growth of the host galaxy, likely fueled by mergers (Hutchings et al. 2006; Hopkins et al. 2006). Studies of the young stellar populations of radio galaxies also suggest merger-driven star-bursts (Tadhunter et al. 2005). Observations of $z \sim 2$ radio galaxies indicate the powerful outflows that will disperse the surrounding ISM (Nesvadba et al. 2006).

To study the process of a quasar emerging from its dusty cocoon, we need transition ultraluminous infrared galaxies (ULIRGs), i.e., containing a quasar still enshrouded by dust (e.g., Canalizo & Stockton 2001). Unlike IR, optical, or X-ray diagnostics, extreme radio luminosity is a dust-independent, unambiguous indicator of a highly obscured active galactic nucleus (AGN; e.g., Martínez-Sansigre et al. 2005; Donley et al. 2005).

We have a sample of *Spitzer*-selected $z \sim 2$ ULIRGs whose continuum-dominated mid-IR spectra already imply the presence of an AGN (Yan et al. 2007; Sajina et al. 2007). In this Letter, we highlight the seven sources of this sample which are radio-loud, confirming the AGN, while their deep 9.7 μm silicate absorption indicates significant obscuration. Throughout this Letter we adopt the ΛCDM cosmology with $\Omega_M = 0.3$, $\Omega_\Lambda = 0.7$, and $H_0 = 70$ km s^{-1} Mpc^{-1}.

2. THE SAMPLE

Our sources are part of a sample of 52 high-z ULIRGs with *Spitzer* Infrared Spectrograph (IRS; Houk et al. 2004) spectra

(Yan et al. 2007). In summary, the sample is selected from the *Spitzer* First Look Survey (FLS). They are selected for having 24 μm flux density brighter than 0.9 mJy, and red 24-to-8 μm and 24-to-R colors.[2] Of these, 47 have IRS-based redshifts, with the majority (33/47 = 72%) at $1.5 < z < 3.2$. The analysis of the IRS spectra and derivation of PAH luminosities, equivalent widths, and silicate feature optical depths[3] ($\tau_{9.7}$) is presented in Sajina et al. (2007). All sources in our sample show evidence of both star formation and AGN activity; however, based on their PAH-strengths versus mid-IR continua, the "weak-PAH" (EW$_{7.7} < 0.8$ μm) sources are believed to be energetically dominated by their AGNs. About 60% of the these weak-PAH sources have significant 9.7 μm silicate absorption with $\tau_{9.7} > 1$. Roughly one-half of these show extreme optical depths ($\tau_{9.7} > 3$). At such high obscurations the IR spectra of AGNs and compact, nuclear starbursts are indistinguishable (Roussel et al. 2006; Levenson et al. 2007). Of the total sample, 60% are detected in the VLA 20 cm map of the FLS (Condon et al. 2003), and 48% are detected in the Giant Metrewave Radio Telescope (GMRT) 610 MHz map of the field (Garn et al. 2007). For a full description of the radio data see A. Sajina et al. (2008, in preparation).

In this Letter, we look only at the 28 $z > 1.5$ continuum-dominated (i.e., likely AGN-dominated) sources. We use their radio emission to reveal the hidden AGNs. We take $L_{1.4\text{GHz}} > 10^{25}$ W Hz^{-1} as our "radio-loud" criterion (e.g., Jiang et al. 2007), while we discuss the more standard radio-to-optical ratio criterion in § 3.4. The seven sources which satisfy this criterion are listed in Table 1 along with a summary of their mid-IR properties from our earlier papers (Yan et al. 2007; Sajina et al. 2007) as well their radio fluxes and luminosities from A. Sajina et al. (2008, in preparation). These seven sources represent 25% of the $z \sim 2$ continuum-dominated sources. For comparison, optically selected quasars have $\sim 10\%$–20% radio-loud fraction (Jiang et al. 2007).

---

[2] (1) $R(24,8) \equiv \log [\nu f_\nu(24 \ \mu\text{m})/\nu f_\nu(8 \ \mu\text{m})] \gtrsim 0.5$;   (2) $R(24,0.64) \equiv \log [\nu f_\nu(24 \ \mu\text{m})/\nu f_\nu(0.64 \ \mu\text{m})] \gtrsim 1.0$.

[3] Our 9.7 μm optical depth is measured from an extinction-corrected continuum and relates to the observed depth of the silicate feature as $\tau_{9.7} = 1.4\tau_{\text{Si}}$ (see Sajina et al. 2007 for details).

---

[1] *Spitzer* Science Center, California Institute of Technology, Pasadena, CA 91125.

SAJINA ET AL.

TABLE 1
SUMMARY OF RADIO-LOUD SAMPLE PROPERTIES

MIPS ID	z	$\tau_{9.7}$	log ($L_{PAH,7.7}$) ($L_\odot$)	log ($L_{14\mu m}$)[a] ($L_\odot$)	$S_{1.4GHz}$ (mJy)	S_{610MHz} (mJy)	α	log ($L_{1.4GHz}$) (W Hz^{-1})
8327	2.48	2.4	10.62 ± 0.21	12.40 ± 0.04	1.40 ± 0.06	3.44 ± 0.14	−1.1	25.89 ± 0.03[b]
15880[c]	1.68	3.9	10.60 ± 0.09	12.51 ± 0.01	0.60 ± 0.03	1.35 ± 0.06	−1.0	25.02 ± 0.14
16059[d]	2.43	2.7	10.76 ± 0.09	12.46 ± 0.02	0.57 ± 0.03	...	...	25.26 ± 0.04
16122	1.97	1.8	10.41 ± 0.21	12.13 ± 0.09	2.82 ± 0.14	4.34 ± 0.12	−0.5	25.66 ± 0.003
22204	2.08	1.6	11.01 ± 0.10	12.63 ± 0.01	1.89 ± 0.08	4.67 ± 0.10	−1.1	25.82 ± 0.004
22558	3.2	>5.6	10.96 ± 0.12	12.88 ± 0.01	0.62 ± 0.03	1.55 ± 0.12	−1.1	25.80 ± 0.02
22277	1.77	1.4	10.44 ± 0.19	12.36 ± 0.05	1.57 ± 0.07	4.79 ± 0.11	−1.3	25.65 ± 0.005

[a] This is monochromatic νL_ν.

[b] This error accounts for the flux error alone; ∼0.2 dex error in α leads to an additional ∼0.1 dex uncertainty.

[c] The radio fluxes for MIPS 15880 are the sum of the three components listed in the respective catalogs; we have checked that there is no significant extended flux missed.

[d] MIPS 16059 is undetected at 610 MHz, since it falls in the noisy edge of the map. We assume $\alpha = -0.7$ for this source.

3. ANALYSIS

3.1. Mid-IR Obscuration

The top panel of Figure 1 shows that all of our radio-loud sources have deep silicate absorption features ($\tau_{9.7} \sim 1$–6). Among our $z \sim 2$ high-τ sources, ∼40% are radio-loud, making this an exceptionally efficient means of selecting high-z radio-loud sources. By contrast, none of the low-τ sources are radio-loud. The observed $L_{14\mu m}$ of the low- and high-τ sources are not significantly different (this holds for L_{FIR} as well; A. Sajina et al. 2008, in preparation). However, the extinction-corrected 14 μm continua are significantly higher for the deeply absorbed sources (Fig. 1, bottom). Higher mid-IR luminosities might indicate any greater black hole masses, greater accretion rates, or more compact dust geometry leading to hotter dust. At present, it is unclear which, if any, of these reasons might explain the lack of radio-loud sources among our low-τ continuum-dominated sources. Shi et al. (2006) show a correlation between
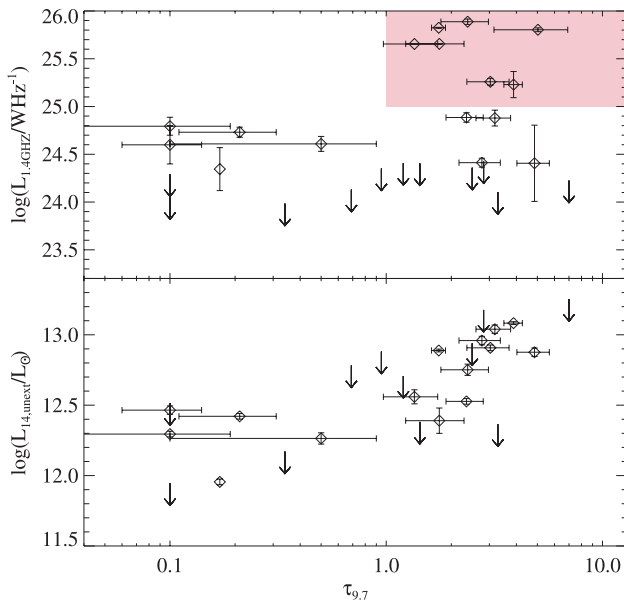

FIG. 1.—Top: 1.4 GHz luminosity vs. 9.7 μm optical depth. For our sample, only sources with strong silicate features ($\tau_{9.7} > 1$) meet the radio-loud criterion ($L_{1.4GHz} > 10^{25}$ W Hz^{-1}). The pink box highlights the region occupied by our seven radio-loud sources. Bottom: Mid-IR continuum luminosity vs. $\tau_{9.7}$. After extinction correction, $L_{14\mu m}$ of the high-τ sources are higher than those of the low-τ sources, possibly providing clues as to why their radio luminosities are higher as well.
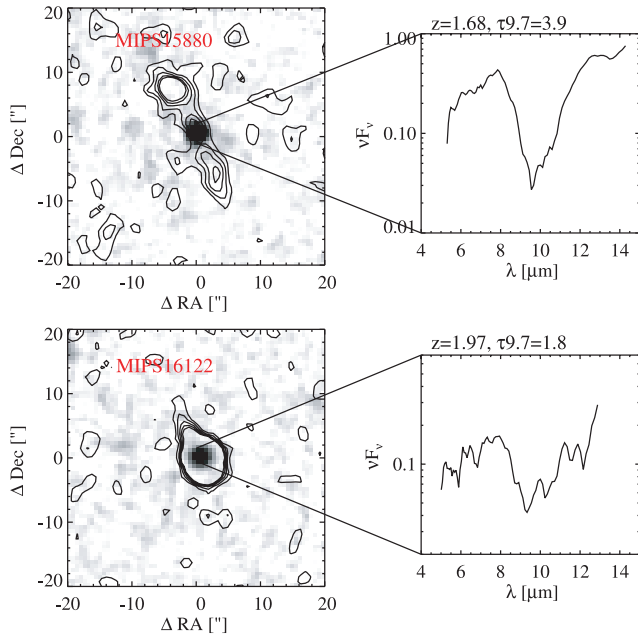
the gas column densities (N_H) and $\tau_{9.7}$. Extrapolating this to the optical depths of our sources, we find $N_H \gtrsim 10^{27}$ cm^{-2}. If confirmed, these sources qualify as Compton-thick quasars. It is, however, likely that this trend breaks down due to differences in the properties and geometry of the obscuring medium (for example, a more uniform, screenlike obscuration as opposed to a more clumpy one). Initial Chandra observations support strong X-ray obscuration (F. E. Bauer et al. 2008, in preparation) given nondetections in 30 ks exposures. Finally, five of the seven meet the Martínez-Sansigre et al. (2005) Compton-thick quasar criteria (MIPS 15880 has too much 3.6 μm flux, while MIPS 16122 has too much 1.4 GHz flux).

3.2. Spectral Indices

The radio spectral indices[4] (α) based on the integrated fluxes at 610 MHz and 1.4 GHz are listed in Table 1. The different resolution of the two images means that the 1.4 GHz map might be missing extended flux relative to the 610 MHz. We estimate the strength of this effect by comparing the α-values based on the integrated or peak 610 MHz fluxes. We find that our α-values can be overestimated by up to ∼0.2 dex. This means up to 0.1 dex overestimation of the radio luminosities, which is not significant for our conclusions. The largest effect is found for our strongest radio source, MIPS 16122, where α ranges between −0.0 and −0.5 for the peak and integrated flux values, respectively. This is our only potentially flat-spectrum source. The typically steep spectra we find are consistent with the $\alpha \sim -1$ of $z \sim 2$ type 2 quasars found by Martínez-Sansigre et al. (2006). Such steep slopes are associated with evolved (i.e., lobe-dominated) radio sources (Martínez-Sansigre et al. 2006), while flat spectra are generally core-dominated sources. Given our radio resolution and the redshifts of these sources, we are only sensitive to extended structures of $\gtrsim 100$ kpc. Below we discuss the two sources with observed radio jets.

3.3. Extended Radio Emission

In § 3.2 we discussed that our spectral indices suggest evolved radio sources. MIPS 15880 shows a transition Fanaroff-Riley type I/II structure with a diameter of ∼200 kpc (see Fig. 2), which is near the mean size for double-lobed structures (de Vries et al. 2006). Given that such moderate-luminosity radio sources have hot spot advance speeds in the range ∼(0.01–0.1)c, this size implies a radio-source age of ∼10^7 yr (e.g., Willott et al. 2002).

The bottom panel of Figure 2 (MIPS 16122) shows the

[4] Defined as $\alpha = \log (S_{610MHz}/S_{1.4GHz})/ \log (610 MHz/1.4 GHz)$.

FIG. 2.—VLA 1.4 GHz contours (1–5 σ) overlaid on the MIPS 24 μm image for MIPS 15880 (*top*) and MIPS 16122 (*bottom*). At the redshifts of both sources the radio beam ($\sim$5″) subtends $\approx$42 kpc. None of the extended structures have counterparts in the *R*-band or IRAC 3.6 μm images. On the right-hand side are shown the IRS mid-IR spectra of both sources. In both cases the redshifts are derived from the silicate feature.

characteristic tadpole shape indicative of a one-sided jet, suggesting that the jet axis is close to the line of sight ($\ll 45°$). It spans $\sim 90/\sin(i)$ kpc, where i is the inclination angle. Higher resolution radio data are, however, required to confirm the morphology of the radio source. We see no counterpart to the extended emission in our *Hubble Space Telescope* (*HST*) NICMOS image (Dasyra et al. 2007).

3.4. *Radio versus Mid-IR Emission*

Figure 3 puts our sources in context with related populations. A number of assumptions were necessary to put the various disparate samples on the same plane (see Fig. 3 legend). These assumptions are crude but acceptable given the dynamic range of this figure.

Does our classification agree with the more common "radio-loud" definition, $R \equiv $ f5 GHz/f4400 Å > 10? Given the significant obscuration of our sources, this definition is not immediately applicable. We translate f4400 Å to f14 μm luminosities based on the average quasar spectrum (Richards et al. 2006b) and assume $\alpha = -0.7$ in the radio, which leads to an equivalent criterion, $R_{\rm IR} \equiv L_{1.4{\rm GHz}}/L_{14\mu m} > 10^{-5}$ (Fig. 3, *dotted line*). Four of our sources remain radio-loud in this definition as well, while three are borderline, although possibly still radio-loud given the rough derivation above. In addition, the screen extinction correction we apply to $L_{14\mu m}$ is likely to overestimate the mid-IR luminosities. With no strong dichotomy between our radio-loud and "radio-quiet" sources, are we not subject to rather arbitrary definitions? Obviously, we see extended emission among the radio-loud sources and not the rest of the sample. Only four of the non–radio-loud sources have detections at 610 MHz, implying a generally flatter radio spectrum than for the radio-loud sources. Finally, there exists a surprising difference between high-τ and low-τ sources (see
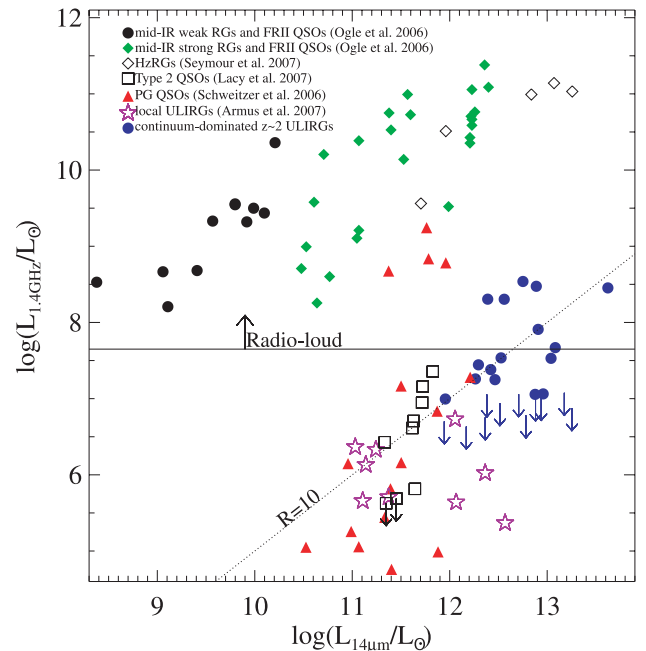

FIG. 3.—Comparison between our sources and other radio-loud or ULIRG populations. Ogle et al. (2006) quote L_{15}, which is close enough to L_{14} for our purposes. The type 2 quasars we plot are all at $z \sim 0.4$–0.8, so that the observed 24 μm flux is close to the rest-frame 14 μm. The high-z radio galaxies (HzRGs) shown are those with both 24 and 70 μm detections (Seymour et al. 2007), we interpolated between these fluxes to derive the rest-frame 14 μm. For both our sample and the ULIRGs, we use extinction-corrected $L_{14\mu m}$. The 1.4 GHz fluxes of the PG quasars, type 2 quasars, and ULIRGs are taken from NED. The 1.4 GHz luminosities assume an $\alpha = -0.7$. The dotted line represents the classic radio-to-optical ratio definition of radio-loud (see text for details).

§ 3.1). These support the view of our radio-loud sources as a distinct population.

3.5. *Black Hole Masses*

The total IR luminosities (~ 3–$4L_{14\mu m}$; A. Sajina et al. 2008, in preparation) are likely $\approx L_{\rm bol}$ for such highly obscured sources. Based on these and assuming Eddington accretion, we estimate black hole masses of $\sim(2$–$6) \times 10^8 M_\odot$. This is supported by the empirical relation between radio luminosity, $M_{\rm BH}$, and accretion rate (Lacy et al. 2001), which leads to $\langle M_{\rm BH} \rangle \sim 3.0 \times 10^8 M_\odot$, again assuming Eddington accretion.

Our sources do not represent a complete census of massive black holes at $z \sim 2$, and are likely to experience further growth between then and $z \sim 0$. With this in mind, can we reconcile such massive black holes at $z \sim 2$ with the space density of massive black holes today? The density of our $z \sim 2$ heavily obscured radio-loud sources is $\sim 3 \times 10^{-7}$ Mpc^{-3}. Lauer et al. (2007) estimate the space density of black holes with $M_{\rm BH} \geq 3 \times 10^8 M_\odot$ (typical of our sources) is $\sim 3 \times 10^{-4}$ Mpc^{-3} locally. This generous gap between the space densities implies we are not overproducing black holes at $z \sim 2$.

4. DISCUSSION

Our study for the first time directly demonstrates the existence of deep silicate absorption ($\tau_{9.7} \sim 1$–6) radio-loud sources at $z \sim 2$. This is in strong contrast with $z \lesssim 1$ radio-loud populations where none have $\tau_{9.7} > 1$ (Haas et al. 2005; Ogle et al. 2006). The high obscurations of our sources is largely a selection bias, as our sample was selected to be mid-IR bright

and red (§ 2). However, *high radio fluxes are not part of our selection*, and hence, the 40% radio-loud fraction of our high-τ $z \sim 2$ sources is a real effect. This implies a direct or indirect coupling between the radio source and surrounding ISM. Weedman et al. (2006) present a $z \sim 2$ sample similar to ours, but including a radio selection. A quick analysis of their sample yields two sources that are both radio-loud and have $\tau_{9.7} > 1$, further supporting our results.

The much greater $L_{14\mu m}/L_{1.4GHz}$ ratios of our sources relative to local radio-loud sources imply that we are observing these sources in the brief window between the birth of the radio source and before feedback effects have shed the dusty envelope and halted the starburst and/or black hole accretion. Willott et al. (2002) argue that the IR-brightness is anticorrelated with the age of the radio source consistent with a radio source–driven feedback scenario. Given the age of MIPS 15880 ($\gtrsim 10^7$ yr), its radio jets are not necessarily powerful enough to accomplish this. But this may be a function of radio luminosity. MRC 1138−262, a $z = 2.2$ radio galaxy more than 2 orders of magnitude more radio-luminous than our sources, does show powerful outflows, which are probably driven by lateral shocks from the radio jets (Nesvadba et al. 2006). A mid-IR study of a sample of $z \sim 2$ radio galaxies, covering a range of radio luminosities, would therefore provide very useful constraints on radio jet–ISM interactions at the epoch when radio galaxies are in the process of shedding their dusty envelopes.

The above does not explain why our sources should have deeper silicate absorption than local radio-loud populations. The answer hinges on the unknown origin of the mid-IR obscuration, e.g., a dusty torus or host galaxy. The deep silicate features of our sources imply optically thick obscuring media with high filling factors (i.e., likely a puffed-up geometry, but not 4π given the radio jets) as they have to effectively "hide" the hot inner regions of the AGN (Pier &

Krolik 1992; Levenson et al. 2007). AGN tori are believed to be clumpy, which precludes high filling factors (Elitzur & Shlosman 2006), consistent with their observed weak silicate features (Shi et al. 2006). Higher $\tau_{9.7}$ can be due to a cold dust screen (Ogle et al. 2006), such as is expected from a dusty host galaxy. High-z radio galaxies/radio-loud quasars have been detected in the submillimeter, indicating cold dust (Willott et al. 2002; Reuland et al. 2003). We already know that the number density of deeply obscured sources is about 10 times higher at $z \sim 2$ than at $z \sim 0$ (Sajina et al. 2007). Finally, MIPS 16122 is consistent with a jet axis close to the line of sight ($\ll 45°$). The dusty torus of an AGN is believed to be coupled with the accretion disk (e.g., Elitzur & Shlosman 2006), implying a nearly face-on torus for MIPS 16122, which is unlikely given its deep silicate absorption feature. On the other hand, a mismatch between the orientation of the host galaxy and AGN is frequently observed (Schmitt et al. 2002). Thus, although the origin of the mid-IR obscuration remains an open question, host galaxy obscuration is a good candidate.

REFERENCES

Armus, L., et al. 2007, ApJ, 656, 148
Beelen, A., Cox, P., Benford, D. J., Dowell, C. D., Kovács, A., Bertoldi, F., Omont, A., & Carilli, C. L. 2006, ApJ, 642, 694
Canalizo, G., & Stockton, A. 2001, ApJ, 555, 719
Condon, J. J., Cotton, W. D., Yin, Q. F., Shupe, D. L., Storrie-Lombardi, L. J., Helou, G., Soifer, T., & Werner, M. W. 2003, AJ, 125, 2411
Dasyra, K., et al. 2007, ApJ, submitted
de Vries, W. H., Becker, R. H., & White, R. L. 2006, AJ, 131, 666
Donley, J. L., Rieke, G. H., Rigby, J. R., & Pérez-González, P. G. 2005, ApJ, 634, 169
Elitzur, M., & Shlosman, I. 2006, ApJ, 648, L101
Garn, T., Green, D. A., Hales, S. E. G., Riley, J. M., & Alexander, P. 2007, MNRAS, 376, 1251
Giavalisco, M., et al. 2004, ApJ, 600, L103
Haas, M., Siebenmorgen, R., Schulz, B., Krügel, E., & Chini, R. 2005, A&A, 442, L39
Hopkins, P. F., Somerville, R. S., Hernquist, L., Cox, T. J., Robertson, B., & Li, Y. 2006, ApJ, 652, 864
Houck, J. R., et al. 2004, ApJS, 154, 211
Hutchings, J. B., Cherniawsky, A., Cutri, R. M., & Nelson, B. O. 2006, AJ, 131, 680
Jiang, L., Fan, X., Ivezić, Ž., Richards, G. T., Schneider, D. P., Strauss, M. A., & Kelly, B. C. 2007, ApJ, 656, 680
Lacy, M., Laurent-Muehleisen, S. A., Ridgway, S. E., Becker, R. H., & White, R. L. 2001, ApJ, 551, L17
Lacy, M., Petric, A., Sajina, A., Canalizo, G., Storrie-Lombardi, L. J., Armus, L., Fadda, D., & Marleau, F. R. 2007, AJ, 133, 186
Lauer, T. R., et al. 2007, ApJ, 662, 808
Levenson, N. A., Sirocky, M. M., Hao, L., Spoon, H. W. W., Marshall, J. A., Elitzur, M., & Houck, J. R. 2007, ApJ, 654, L45

Magorrian, J., et al. 1998, AJ, 115, 2285
Martínez-Sansigre, A., Rawlings, S., Garn, T., Green, D. A., Alexander, P., Klöckner, H.-R., & Riley, J. M. 2006, MNRAS, 373, L80
Martínez-Sansigre, A., Rawlings, S., Lacy, M., Fadda, D., Marleau, F. R., Simpson, C., Willott, C. J., & Jarvis, M. J. 2005, Nature, 436, 666
Nesvadba, N. P. H., Lehnert, M. D., Eisenhauer, F., Gilbert, A., Tecza, M., & Abuter, R. 2006, ApJ, 650, 693
Ogle, P., Whysong, D., & Antonucci, R. 2006, ApJ, 647, 161
Pier, E. A., & Krolik, J. H. 1992, ApJ, 401, 99
Reuland, M., van Breugel, W., Röttgering, H., de Vries, W., De Breuck, C., & Stern, D. 2003, ApJ, 582, L71
Richards, G. T., et al. 2006a, AJ, 131, 2766
———. 2006b, ApJS, 166, 470
Roussel, H, Helou, G., Smith, J. D., et al. 2006, ApJ, 646, 841
Sajina, A., Yan, L., Armus, L., Choi, P., Fadda, D., Helou, G., & Spoon, H. 2007, ApJ, 664, 713
Schmitt, H. R., Pringle, J. E., Clarke, C. J., & Kinney, A. L. 2002, ApJ, 575, 150
Schweitzer, M., et al. 2006, ApJ, 649, 79
Seymour, N., et al. 2007, ApJS, 171, 353
Shi, Y., et al. 2006, ApJ, 653, 127
Tadhunter, C., Robinson, T. G., González Delgado, R. M., Wills, K., & Morganti, R. 2005, MNRAS, 356, 480
Wall, J. V., Jackson, C. A., Shaver, P. A., Hook, I. M., & Kellermann, K. I. 2005, A&A, 434, 133
Weedman, D. W., Le Floc'h, E., Higdon, S. J. U., Higdon, J. L., & Houck, J. R. 2006, ApJ, 638, 613
Willott, C. J., Rawlings, S., Archibald, E. N., & Dunlop, J. S. 2002, MNRAS, 331, 435
Yan, L., et al. 2007, ApJ, 658, 778